

Randomized and Efficient Time Synchronization in Dynamic Wireless Sensor Networks: A Gossip-Consensus-Based Approach

Nan Xiong ¹, Minrui Fei ^{1*} and Taicheng Yang ²

¹ Shanghai Key Laboratory of Power Station Automation Technology, School of Mechatronics Engineering and Automation, Shanghai University, Shanghai 200072, China; nan0521@i.shu.edu.cn (N.X.)

² Department of Engineering and Design, University of Sussex, Brighton BN1 9QT, U.K.; taiyang@sussex.ac.uk (T.Y.)

* Correspondence: mrfei@staff.shu.edu.cn (M.F.); Tel.: +86-021-5633-1934

Academic Editor: name

Version August 4, 2018 submitted to Complexity;

Abstract: This paper proposes novel randomized gossip-consensus-based sync (RGCS) algorithms to realize efficient time correction in dynamic wireless sensor networks (WSNs). First, the unreliable links are described by stochastic connections, reflecting the characteristic of changing connectivity gleaned from dynamic WSNs. Secondly, based on the mutual drift estimation, each pair of activated nodes fully adjusts clock rate and offset to achieve network-wide time synchronization by drawing upon the gossip consensus approach. The converge-to-max criterion is introduced to achieve a much faster convergence speed. The theoretical results on the probabilistic synchronization performance of the RGCS are presented. Thirdly, a Revised-RGCS is developed to counteract the negative impact of bounded delays, because the uncertain delays are always present in practice and would lead to a large deterioration of algorithm performances. Finally, extensive simulations are performed on the MATLAB and OMNeT++ platform for performance evaluation. Simulation results demonstrate that the proposed algorithms are not only efficient for synchronization issues required for dynamic topology changes but also give a better performance in term of converging speed, collision rate, and the robustness of resisting delay, and outperform other existing protocols.

Keywords: wireless sensor networks; consensus time synchronization; gossip algorithms; changing connectivity; fast convergence; collisions; bounded delays;

1. Introduction

Ad hoc Wireless Sensor Networks (WSNs) without pre-existing infrastructures are composed of autonomous sensors [1], and the sensors are a variety of low cost, low power, sensing devices, which work cooperatively through ad hoc wireless communications. In WSNs, many kinds of missions [2,3], such as transmission scheduling, event sequencing, information fusion, and distributed filtering, rely heavily on a consistent notion of time to keep running. For instance, Internet of Things' perception layer provides a ubiquitous access to the network, in which the multiple terminals collaborate closely with each other, and accurate synchronized clocks determine whether a multi-terminal cooperation is accomplished or not. Therefore, timing protocols, which should concern with topologies, time-delays, low power consumption, etc., is the premise of dealing with services of ad hoc WSNs.

Two configurations of timing protocols are available: hierarchical and distributed. Cluster-based and tree-based protocols would both fall into the hierarchical configuration, because they perform a special operation; that is, some designated nodes are elected to be the reference (such as cluster head, root, master). The typical hierarchical timing protocols include the one-way message dissemination schemes [4], two-way message exchange schemes [5], flooding schemes [6], Pairwise Broadcast

32 Synchronization (PBS) [7], and Reference Broadcast Synchronization (RBS) [8]. Based on the message
33 passing and filter methods, most of the works have build an estimation and tracking framework for
34 the time synchronization problem, but these prototypes are not purely decentralized in nature. The
35 hierarchy structure of network consists in the logical master-slave relationship which is maintained
36 by actual infrastructure. The timing messages in this structure are delivered from top to bottom, while
37 each node is labeled an equal identity tag in distributed configuration. In the absence of pre-existing
38 infrastructure, the distributed configuration is obviously more suitable to WSNs.

39 Recently, based on distributed consensus algorithms [9,10] of multi-agent networks, consensus
40 based approaches for designing distributed timing protocols [11–21] have received a lot of attention in
41 WSNs. These protocols utilize local information to achieve global synchronization and easily adopt to
42 WSNs' distributed sensor property with computational lightness. However, the common drawbacks
43 of existing consensus based timing protocols are as follows:

44 (1) The changing connectivity is rarely considered [17]. In dynamic WSNs, it is not possible to
45 deterministically forecast the activating timeslot of sensors due to the uncertainties of nodes, such
46 as uncontrollable mobility, sleep scheduling, heterogeneous nodes with various coverage levels, etc.
47 Radio signal fading caused by environmental turbulence can also severely corrupt the performance of
48 wireless links. The nodes in the design of the consensus based timing protocols sequentially update
49 their own clocks whenever they receive a timing message from a geographical neighbor [11]. Because
50 the logical rate represents the slope of the linear logical clock model, each node i is required to build a
51 fixed link with a same neighboring node in order to collect timing messages and estimate the relative
52 drift. In the MTS [12], the authors assume that a larger B is used to keep link (i, j) constant during a
53 time interval $[kB, (k + 1)B]$. Although it enables the MTS to behave robustly to work against topology
54 changes, in highly dynamic topology this assumption will be unrealistic. This is because at a timeslot
55 t_1 , node i can exchange timing messages with a neighbor only once to obtain clock reading. At next
56 timeslot t_2 , the link (i, j) will lost the connection. More generally, any pair of nodes "gossip" only once
57 in one timeslot. Thus, the randomly changing connectivity between adjacent nodes renders efficient
58 relative drift estimation challenging. This problem will directly affect the implementation of logical
59 clock rate and offset compensation, and become more paramount as the change of connected relation
60 of WSNs gets faster. On this issue the existing consensus based timing protocols can be classified into
61 two categories: 1) deterministic synchronization, which relies on a fixed link, such as [11–18]; and 2)
62 randomized synchronization, such as [19–21]. Brown et al. [19] investigated the transient consensus
63 behavior of the Random Pairwise Consensus Synchronization (RPCS) algorithm. It is a pity that the
64 reciprocal delay model is supposed to be symmetric. Strom et al. [20] proposed a randomized method
65 to deal with the random access problem. The method proposed therein combines partial-update rule
66 with complete-update rule. However, the partial-update rule is capable of compensating the offset in
67 non-deterministic instants which results in incompletely compensating the clock rate. Bolognani et
68 al. [21] proposed a randomized linear algorithm for the second-order consensus timing protocol. This
69 algorithm is based on the average-value-based criterion, which have a slow speed of convergence.

70 (2) The speed of convergence may be relatively slow. A major concern is the lower convergence
71 speed which increases the message complexity and consumes the limited power of the sensor nodes.
72 However, many protocols [11,13–16,19–21] are proposed based on the average-value-based criterion,
73 which need more iterations to achieve acceptable synchronization error.

74 (3) The delay model is unrealistic. Several protocols suppose the uplink delay and the downlink
75 delay among two nodes are symmetric [13,19] or obey a statistical delay model [12,14], such as normal
76 distribution, Gaussian distribution, etc. Worse still, the uncertainty regarding the delay is associated
77 with the influence of exterior environment.

78 (4) The common broadcast period would give rise to the timing message collision as pointed out
79 in publications [11,18,20], but without being handled. The existing consensus based timing protocols
80 employ a deterministic communication protocol, in which each node is allowed to communicate with
81 its neighboring nodes that are within its range in each deterministic timeslot. Due to the hidden node

82 problem [24], the collisions become too serious to be further ignored since a exposed node receives
83 multiple timing messages from hidden nodes with common broadcast period during a same timeslot.

84 The critical fact that the real-world delays would change irregularly, and the more iterations and
85 the collisions would waste energy, has a negative effect on synchronization performances.

86 Inspired by the rumor spreading of human groups and the way how epidemics spread, gossip
87 algorithm [25,26] has been widely investigated in the information theory community for information
88 dissemination. In the context of the multi-agent networks, randomized gossip algorithm is attractive
89 for solving the distributed and stochastic consensus problems [27–29] due to its randomized behavior
90 and asynchronous processing. Faced with the dynamic topology issue, the gossip consensus provides
91 less conservatism and higher efficiency than the existing consensus approach. So they are perceived
92 as uniquely suited for the inherent dynamics of ad hoc WSNs whose topology is randomly connected.
93 The gossip consensus approach contains two dimensions: gossip interaction and gossip update. The
94 gossip interaction mode is particularly well suited for applications into wireless peer-to-peer and ad
95 hoc sensor networks, where a random pair of nodes is active at each iteration and out-sync itself is a
96 prior fact. In addition, randomized gossiping may allow communication asynchronously at random
97 times to lower the probability of message collisions. The gossip update policy is that each node has to
98 share its output with one of neighboring nodes. That being said, privacy issues could easily apply to
99 a node who participating in such updating. On the contrary, the existing consensus approach allow
100 a node to share its output with multiple nodes, so privacy issues could discourage some nodes from
101 participating in such updating. Therefore, under a more practical delay model, it is of great interest
102 to study randomized gossip algorithm for achieving the generalized consensus timing protocol that
103 has faster convergence speed and lower collision rate in dynamic WSNs.

104 Motivated by these, this paper presents an innovative randomized and efficient timing protocol
105 for dynamic WSNs, including the mutual drift estimation, the clock rate and offset compensation.
106 The key novelty of the contribution lies in randomized algorithm for the extension of the generalized
107 consensus based timing protocol which implements probabilistic synchronization using randomized
108 gossip-type interactions and updates. To achieve this goal, for the first time, we design the idea of the
109 randomized activation of the synchronization links based on the pre-programmed Poisson process
110 to activate a pair of nodes, and use the gossip-consensus-based approach with the converge-to-max
111 criterion to fully adjust the clock rate and offset of random pairwise nodes. Moreover, by exploiting
112 a least square based low-pass filter, a revised version is improved to cope with the bounded delays.

113 The major contributions of this paper are summarized below:

- 114 • We first ignore the time-delays and propose a novel Randomized Gossip-Consensus-based time
115 Synchronization (RGCS) protocol by incorporating the idea of randomized gossip algorithm into
116 the consensus based timing protocol. Compared to traditional mechanisms, the gossip consensus
117 is achievable in a fully decentralized, randomized and asynchronous fashion, even in highly
118 dynamic WSNs. The converge-to-max criterion is introduced to achieve finite-time convergence,
119 since the gossip consensus is a not fast convergence algorithm. Then we prove that the expected
120 logical clocks are synchronized with probability one (w.p.1), and provide a lower bound of fast
121 finite-time convergence. In addition, we develop Multi-RGCS protocol based on the principle of
122 the Edge-Coloring (EC) technique to save finite-convergence time.
- 123 • We consider the case where the delay obeys a realistic bounded model compared to the particular
124 distribution communication delay model, and further propose a Revised-RGCS protocol to work
125 against the uncertain bounded time-delays. The filter proposed therein is competent to deal with
126 practical delays which could be a basic constraint in drift estimation issue over real-world WSNs.
- 127 • We conduct performance evaluations of the proposed protocols through extensive simulation
128 experiments using the MATLAB and OMNeT++. Simulation results demonstrate that RGCS fully
129 adjusts logical rate and offset to achieve network-wide synchronization for randomly connected
130 WSNs, and Revised-RGCS gives a better performance in terms of collision rate, converging speed,
131 and the robustness of resisting delays compared to other existing protocols.

132 The rest of this paper is organized as follows. In section 2, we review the related literatures and
133 state the novelty with respect to the previous works. Section 3 formulates the time synchronization
134 problem. Section 4 elaborates the proposed RGCS, Multi-RGCS, and Revised-RGCS. The simulation
135 results are given in Section 5. Section 6 concludes the paper.

136 2. Related Work

137 In the absence of pre-existing infrastructures, distributed configuration is a promising paradigm
138 for distributed WSNs. Within this context, tremendous research efforts have already been devoted
139 to distributed timing protocols. Based on belief propagation, a fully distributed timing protocol [30]
140 developing from the two-way sender-receiver synchronization scheme was used for joint estimation
141 of rate and offset. Distributed asynchronous Clock Synchronization (DCS) [31] protocol was proposed
142 for delay-tolerant networks. DCS can achieve global time synchronization among mobile nodes over
143 intermittent connections with long delays, but the rate and offset are adjusted separately. Ahmed et al.
144 [32] considered unreliable links to build asynchronous framework, but it is the same as RFA without
145 rate compensation. An On-demand Time Synchronization Protocol (AOTSP) [33] was proposed with
146 the advantages of weak spatial accumulative effect, low communication cost, and high scalability.
147 However, AOTSP suffers from temporal accumulative effect on account of exchanging timestamps.

148 In recent years, distributed consensus concept [9,10] has become a hot topic in the distributed
149 time calibration research. Distributed timing protocol based on the idea of the consensus algorithm
150 was originally achieved with the Average TimeSynch (ATS) [11] protocol which fully compensates
151 clock rate and offset. To accelerate convergence speed, the Maximum Time Synchronization (MTS)
152 [12] protocol was developed by which the system trajectories of rate and offset are updated to achieve
153 maximum-value under normal distribution delay model, and Saiah et al. [14] proposed Consensus
154 based Multi-hop Time Synchronization (CMTS) protocol under Gaussian delay model. Panigrahi
155 et al. [13] proposed a multi-objective evolutionary strategy based topological optimization for the
156 consensus timing protocol to deal with a trade-off between the minimizing of delays and the selection
157 of sync initiating nodes, but the delays are assumed to be symmetric. The other improved protocols
158 include the Robust-ATS (RoATS) [15] and Least Square estimation based Time Synchronization (LSTS)
159 [16] aiming at the delays. Recent works contributed by Tian et al. [17] presented a very generalized
160 model of Consensus Based Time Synchronization (CBTS) algorithm without topological conditions.
161 However, the RoATS, LSTS, and CBTS designed for distributed WSNs with delays are static scenarios
162 and ignore the changing connectivity of dynamic WSNs. Brown et al. [19] investigated the transient
163 consensus behavior of clock parameters in the Random Pairwise Consensus Synchronization (RPCS).
164 Similar to DCS, RPCS adjusts rate and offset separately. He and Dong et al. investigated consensus
165 timing protocol under message manipulation attacks [22] and sybil attacks [23], respectively. In order
166 to address topology change issue, the MTS protocol suppose that link (i, j) should be keep constant
167 within a time width B , however in highly dynamic topology, this assumption is unrealistic. Strom
168 et al. proposed Random Broadcast based Distributed time Synchronization (RBDS) [20] protocol
169 based on random access mechanism, which combines partial-update rule with complete-update rule.
170 However, the partial-update rule is capable of compensating the offset in non-deterministic timeslot
171 which results in incompletely adjusting the drift. Based on the gossip consensus, we relax the basic
172 condition of the MTS (i.e., compared with the MTS, we don't need link (i, j) keep constant during a
173 width of time $[kB, (k + 1)B]$ to collect the clock states more than once) and also enable complete-rate
174 and complete-offset compensation.

175 There has been a surge of activity in ad hoc WSNs using the idea of gossip protocols. Specific to
176 time synchronization, Marechal et al. [34] proposed a distributed gossip protocol for only adjusting
177 natural clock drifts. Ruggero et al. proposed a Proportional Integral (PI) synchronization controller
178 [35] with gossip communication mode for time synchronization. The PI controller proposed therein
179 takes advantage of the asynchronism of pairwise-exchange communication. Coupling-based internal
180 Clock Synchronization (CCS) [36] which combines gossip paradigm with a nature-inspired approach

181 was proposed to cope with disturbance. The logical clock in the CCS is equal to the hardware clock
 182 plus an adjustment. This is a special case of our logical clock model which has both multiplicative and
 183 additive compensation. Joerg et al. [37] proposed a hybrid protocol for distributed microphones over
 184 a wireless network, in which integrated the two-way message exchange mechanism with gossiping
 185 technique. The idea of gossiping used therein mainly seeks a virtual master clock. Based on broadcast
 186 gossiping, Stankovic et al. [38] proposed two instrumental variable type distributed recursions for
 187 estimating parameters of calibration functions with a general noise assumption. A concern regarding
 188 distributed recursion is their excessive use of communication, while the nodes of randomly connected
 189 networks can only communicate with its immediate neighbor in an opportunistic manner.

190 In summary, some of the above algorithms only compensate offset or rate [29,32,34], and other
 191 algorithms compensate offset and rate separately [4,19,31,37]. Several algorithms reconstruct clock
 192 parameters and perform reverse reconstruction to align absolute time, so they usually introduce more
 193 computational complexity [4,32,37]. The distributed nature of the consensus based timing protocols is
 194 superior to other timing protocols, but the message collision rate is relatively high. In particular, node
 195 i announces a timing message when the hardware clock τ_i or logical clock T_i is such that there exists
 196 an integer Ψ satisfying $\tau_i(t) = n\Psi$ or $T_i(t) = n\Psi + \phi_i$, $n = 1, 2, 3, \dots, N$. There is a high probability
 197 of a timing message collision event in algorithmic mechanisms when the hardware parameters or
 198 bias ϕ are closely for at least two unidentified and hidden nodes [11,12,18,20,23]. In addition, many
 199 algorithms [11,13–16,18–21,34] are still average-value-based algorithms, which have a slow speed of
 200 convergence. Worse still, under significant clock drifting, the average information will remove after
 201 few iterations with a slow speed of convergence. Hence, taking the above reasons into consideration,
 202 energy-efficient time synchronization for dynamic WSNs may not be achieved by these consensus
 203 based timing protocols. The major advantage of the gossip idea is that the iterative dynamics appear
 204 as randomized and asynchronous evolution, so that it is quite convenient for asynchronous network
 205 and topological changes. Nevertheless, the main drawbacks of the aforesaid gossip-based protocols
 206 have been analyzed from the compensation quantity, the excessive use of communication, etc.

Table 1. The comparison of representative distributed timing protocols

	Dynamic topology	Delay	Iterative way	Interference	Rate	Offset
MTS [12]	Yes	Yes	Max	High	Yes	Yes
RoATS [15]	No	Yes	Average	High	Yes	Yes
RPCS [19]	Yes	Yes	Average	High	Separate	Separate
RBDS [20]	Yes	No	Average	High	Incomplete	Yes
RFA [29]	No	No	-	Low	No	Yes
DCS [31]	Yes	Yes	Average	High	Separate	Separate
AOTSP [33]	No	Yes	-	Low	Yes	Yes
CCS [36]	No	Yes	Average	Low	No	Yes
Ours	Yes	Yes	Max	Low	Yes	Yes

207 So, taking a hybrid approach, we first proposed RGCS algorithm without considering the delays,
 208 which combines the advantage of randomized gossip algorithm and consensus based timesync. The
 209 algorithm fully adjusts rate and offset, and also fits into the dynamic topology of randomly connected
 210 WSNs with lower collision. The converge-to-max criterion was introduced to choose the coefficients
 211 properly in order to enable fast convergence. A Revised-RGCS algorithm was developed by adopting
 212 the least square based low-pass filter to counteract the impact of bounded delays. Summing up the
 213 works for comparison in this section, the features of representative distributed timing protocols are
 214 summarized in Table 1. Our time synchronization properties include:

- 215 • Rate and offset synchronization. Each clock rate and offset should be fully adjusted to achieve a
216 common virtual clock.
- 217 • Compatible with dynamic topology changes. A time synchronization protocol has to explore the
218 changing connectivity to design compensation rules.
- 219 • Energy-efficient. The number of message collisions should be small. Synchronization should be
220 finished within a limited time, since the gossip consensus is a not fast converging algorithm.
- 221 • Robustness against bounded time-delays. The bounded convergence should be guaranteed even
222 when bounded uncertain delays are present.

223 3. Problem Formulation

224 Suppose N sensor nodes of a WSN indexed by $i = 1, 2, \dots, N$. Owing to the node dormancy or
225 death and random failure of links, a successful contact between a pair of nodes i and j depends on the
226 probability distribution of the setup of stochastic links. Thus, the topology of dynamic ad hoc WSNs
227 is modeled as a time-varying graph $\mathcal{G}(t) = (\mathcal{V}, \mathcal{E}(t))$. \mathcal{V} is the set of vertices, and the existence of
228 stochastic links $\mathcal{E}(t) = \{e_{ij}(t) | i, j \in \mathcal{V}\}$ is determined independently. The set of node i 's neighbors is
229 denoted by $\mathcal{N}_i = \{j \in \mathcal{V}, e_{ij} \in \mathcal{E}(t)\}$. We use a notation (ij) to indicate e_{ij} which means node i and j
230 happen to link together, and the undirected random graph is bidirectional.

231 **Definition 1.** A synchronization link (ij) or e_{ij} means that an arbitrary random node i is coupled
232 with its geographical neighbor $j \in \mathcal{N}_i$ once to perform synchronous operation. Specifically, triggering
233 node i sends a beacon to choose the triggered neighbor j and confirm the ID of the synchronization
234 link e_{ij} , then they swap timing messages with each other. Due to the randomized activation of nodes,
235 we need neighbor discovery protocol for nodes to discover each other when they are neighbors.
236 Fortunately, a simple and useful neighbor discovery protocol can be used as in [39].

237 **Assumption 1.** When node $i (i \in \mathcal{V})$ is activated at time t , the cardinality $|\mathcal{N}_i(t)| \geq 1$.

238 **Assumption 2.** The delays of the l th uplink and downlink communication between node i and
239 j is denoted by d_{ij} and d_{ji} . They are unequal and bounded by upper bound D ; that is, $0 < d_{ij} < D$,
240 $d_{ij} \neq d_{ji}$.

241 The oscillator generates the standard unit of frequency Ω . The clock provides its reading $\tau(t)$ of
242 the elapsed absolute time t by accumulating the number of impulsive signals $\tau(t) = \kappa \int_{t_0}^t \Omega(\epsilon) d\epsilon +$
243 $\tau(t_0)$, where κ is a oscillator frequency correction. The oscillation frequency is nearly invariable in a
244 short time horizon, so the clock reading of the i th node possesses linear dynamic behavior such as

$$245 \tau_i(t) = a_i t + b_i, \quad (1)$$

246 where a_i, b_i is the hardware clock rate and offset, respectively. a_i determines the timing rate of clock
247 and b_i represents the difference of nodes' clock reading. The logical clock is a linear affine function of
248 $\tau_i(t)$. $\alpha_i(t)$ is a multiplicative compensation and $\beta_i(t)$ is an additive compensation, as follows

$$249 T_i(t) = \alpha_i(t) \tau_i(t) + \beta_i(t) = \tilde{\alpha}_i(t) t + \tilde{\beta}_i(t), \quad (2)$$

250 where $\tilde{\alpha}_i(t) = a_i \alpha_i(t)$, $\tilde{\beta}_i(t) = \alpha_i(t) b_i + \beta_i(t)$ are called the logical rate and offset, respectively. So, we
251 have available quantity $\tau_i(t)$, and two variables $\alpha_i(t), \beta_i(t)$ to be designed.

252 The objective is to design a randomized communication protocol and a gossip-consensus-based
253 approach for coupled nodes $i, j \in \mathcal{V}$ announcing its timing messages and adjusting the logical rate
254 and offset, such that the logical clocks $T_i (i \in \mathcal{V})$ is synchronized in the probability sense, as follows

$$255 \forall i, j \in \mathcal{V}, \exists \Pr \left\{ \lim_{t \rightarrow \infty} [T_i(t) - T_j(t)] = 0 \right\} = 1. \quad (3)$$

256 Finally, notation \Pr, o, \mathcal{O} denote probability, infinitesimal of higher order and infinitesimal of the
257 same order, respectively.

255 4. RGCS, Multi-RGCS, and Revised-RGCS Algorithms

256 4.1. RGCS Algorithm

257 4.1.1. Randomized Communication Protocol

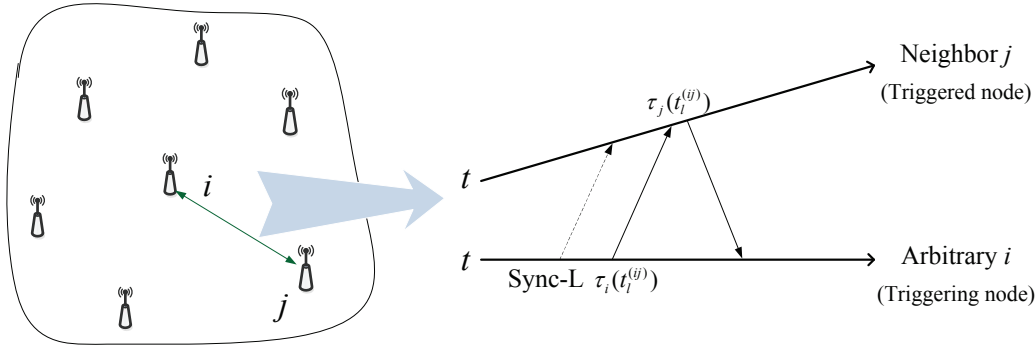


Figure 1. The Sync-L beacon and timing message exchanges in a dynamic wireless sensor network.

258 A randomly connected ad hoc WSN is specifically characterized in that the nodes are randomly
 259 activating and sleeping, and the RGCS algorithm is supposed to run independently in each individual
 260 node. Firstly, the Poisson process is configured to each node in order to generate the Synchronization
 261 Links (Sync-L) beacon which is sent to a node of its neighborhood by exploiting the broadcast nature
 262 of wireless communications. Thus, the randomized activation of $e_{ij}(i, j \in \mathcal{V})$ satisfies Poisson process
 263 with the constant intensity λ_{ij} such that $\Pr\{t^{(ij)}(l + \sigma) - t^{(ij)}(\sigma) = n\} = (\lambda_{ij}l)^n / n! e^{-\lambda_{ij}l}$, $n = 0, 1, \dots$,
 264 for $\forall l, \sigma \geq 0$. Some special circumstances are as follows, if $\lambda_{ij} = 0$, it means link e_{ij} is not activated
 265 forever; if $\lambda_{ij} = \infty$, it means link e_{ij} is activated infinitely in a given time interval. The Sync-L beacon
 266 between node i and j is confirmed, which is referred to the stochastic link activation event. Once
 267 the randomized activation of link e_{ij} takes place, by using the Media Access Control (MAC) layer
 268 time stamps, triggering node i pushes a multivariable message $[\alpha_i(t_i^{(ij)}), \beta_i(t_i^{(ij)}), \tau_i(t_i^{(ij)})]$ to node j .
 269 After that, the triggered node j pulls a multivariable message $[\alpha_j(t_j^{(ij)}), \beta_j(t_j^{(ij)}), \tau_j(t_j^{(ij)})]$ to node i . The
 270 overall procedure is illustrated in Figure 1.

271 Thus, accordingly, the set of activated synchronization links $\{\cup_{i=1, j=1}^N e_{ij}(t)\}$ are an identically
 272 and independently distributed (i.i.d) Poisson distribution. Suppose that function $\mathcal{F}(N)$ represents
 273 the amount of synchronization links of an underlying graph. When it is a complete graph, we can
 274 maximize $\mathcal{F}(N)$ as $N(N - 1)/2$. Clearly, the set $\{\cup_{i=0}^{\infty} \cup_{i=1, j=1}^N t_i^{(ij)} | e_{ij} \in \mathcal{E}(t)\}$ satisfies global Poisson
 275 distribution with the intensity $\mathcal{F}(N)\lambda$, because all intensities have the same value. Each global gossip
 276 instant corresponds to an updating event. We denote $\Delta(l, (ij))$ as the inter-time between consecutive
 277 gossip instants for global Poisson process, and $\{\Delta(l, (ij))\}_{l \in N, (ij) \in \mathcal{E}(t)}$ is an i.i.d process with moments

$$\begin{cases} E[\Delta(l, (ij))] = \frac{1}{\mathcal{F}(N)\lambda} \\ E[\Delta^2(l, (ij))] = \frac{2}{(\mathcal{F}(N)\lambda)^2} \end{cases} \quad (4)$$

278 The intensity λ increased, whereas $\Delta(l, (ij))$ continuously decreased. The physical significance
 279 of λ_{ij} represents the intermittent of activation events of link e_{ij} , and the mathematical meaning of λ_{ij}
 280 represents the mean value of the occurrence of the activation events per unit time. In many scenarios,
 281 environmental-temperature variations will be slow to change around nodes. Hence, we can do that
 282 by increasing intensity λ_{ij} to enlarge the frequency of a link activation event in order to work against
 283 slowly changing drifts.

284 As shown in Figure 2, we illustrate how the proposed mechanism works under the hidden node
 285 problem. Node A is visible from node B, and node C is visible from node B too. However, node A
 286 and node B cannot sense with each other, because they are out of communication zone of each other.
 287 In the deterministic communication protocol (such as ATS, MTS, RoATS, etc.), each node transmits its
 288 timing messages periodically with a common period based on its own clock on chip. If node A and B
 289 have small difference in term of the hardware rate and offset, they will announce timing messages to
 290 node C simultaneously. Thus, the collisions will occur endlessly. In our proposed mechanism, each
 291 node announces a timing message asynchronously based on its pre-programmed Poisson process,
 292 and random pairwise nodes delivery timing messages in the uplink and downlink successively. So
 293 node A randomly gossip, then a sync timeslot is established between node A and C with probability
 294 $\Pr(t_i^{AC})$. The sync timeslot between node B and C is established with probability $\Pr(t_i^{BC})$. The Poisson
 295 intervals δ_{AC}, δ_{BC} are independent of each other. If the transmission delay is negligible, the width of
 296 the sync timeslot can be narrow such that the probability of collisions will further down. Hence, with
 297 an appropriate λ , the probability of collisions is lower than that in the deterministic communication.

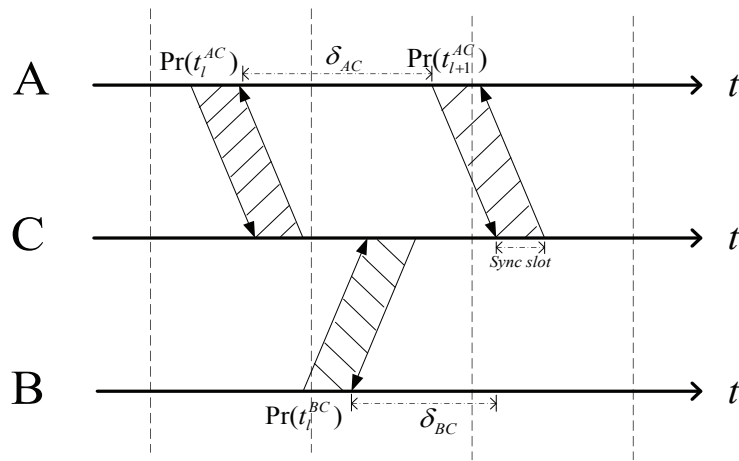


Figure 2. Illustration of the proposed randomized communication under the hidden node scene.

298 To defend against message manipulation attacks, secure consensus timing protocols should
 299 contain detecting and excluding outliers mechanism for the logical clock checking and hardware clock
 300 checking. From the analysis of logical clock checking mechanism in literature [22], we know that the
 301 bounded communication cycle which determined by $\{\Psi|\tau_i(t) = N\Psi, N = 1, 2, \dots, \Psi > 0\}$ is a pivotal
 302 parameter of the secure protocols. However, the authors suppose Ψ is invariable under malicious
 303 modification with the purpose of preventing the attack nodes using outdated receiving information
 304 to cheat, i.e., it makes nodes to collect messages from neighboring nodes within a constant duration.
 305 The proposed gossip interaction mode which has less conservatism to topology changes can remove
 306 this limitation properly. Also, Ψ is the key parameter which contributes to represent the conforming
 307 relationship of Definition 1 in literature [23] to defend against sybil attack, and RGCS is robust to the
 308 distortion of bounded communication cycle.

309 4.1.2. Gossip Consensus Approach for Clock Rate and Offset Compensation

310 Let $\Delta S_i^{(ij)}$ be the difference of hardware clock readings τ_i of triggering node i in gossip instant $t_i^{(ij)}$
 311 and $t_{i-1}^{(ij)}$, namely $\Delta S_i^{(ij)} = \tau_i(t_i^{(ij)}) - \tau_i(t_{i-1}^{(ij)})$. The main idea of the updating rule is to utilize the gossip
 312 consensus approach based on the interchange of the gossiping neighbors' messages. Triggered node
 313 j updates its logical rate $\tilde{\alpha}_j(t)$ and offset $\tilde{\beta}_j(t)$ by averaging them with the estimates of its gossiping
 314 neighbors, namely $\tilde{\alpha}_j(t_{i+1}^{(ij)}) = (1 - \rho_1)\tilde{\alpha}_j(t_i^{(ij)}) + \rho_1\tilde{\alpha}_i(t_i^{(ij)})$. Each node consists of estimating the logical
 315 rate with respect to virtual consensus rate, and local node j stores a new compensation α_j . Then by
 316 dividing α_j at both sides of above equation, we have

$$\alpha_j(t_{l+1}^{(ij)}) = (1 - \rho_1)\alpha_j(\tilde{t}_k^j) + \rho_1(a_i/a_j)\alpha_i(t_l^{(ij)}). \quad (5)$$

317 where $\rho_1 \in (0, 1]$. The constant ρ_1 defines the degree of change of compensation α in gossip instant
 318 $t_{l+1}^{(ij)}$. If ρ_1 is set to a small value, the average information will remove in few updates. Additionally,
 319 due to the discrete observations of the relative drift, we can increase ρ_1 to guarantee stationarity of the
 320 estimated α . Based on the above analysis, the converge-to-max criterion is applied to \tilde{t}_k^j . The time, \tilde{t}_k^j
 321 indicates the previous gossip instant of arbitrary edges who contain node j just before activated edge
 322 e_{ij} 's l th gossip instant. Equation (5) counts the absolute time on two scales, i.e., updating usage round
 323 and communication round, to avoid confusion between the updating iteration and the gossiping
 324 communication. Scrupulously, \tilde{t}_k^j is given as follows

$$\tilde{t}_k^j = \max\{t_s^{(jp)}, t_r^{(qj)} \mid t_s^{(jp)} < t_l^{(ij)}, t_r^{(qj)} < t_l^{(ij)}; p, q = 1, \dots, n; s, r = 1, 2, \dots\}. \quad (6)$$

325 When the Sync-L e_{ij} is activated in the next gossip instant $t_l^{(ij)}$, node i use $\tau_i(t_{l-1}^{(ij)})$ which be stored
 326 in flash memory of sensors to compute the number of drift, namely the relative drift $\alpha_{ji}(t_l^{(ij)})$ for node
 327 j is computed by

$$a_i/a_j = \alpha_{ji}(t_l^{(ij)}) = \Delta S_i^{(ij)} / \Delta S_j^{(ij)}. \quad (7)$$

328 During all iterations, each node i 's storage is $O(|\mathcal{N}_i|)$ for all possible synchronization links. It implies
 329 that, even though the size of the network node increases, the storage complexities of the RGCS per
 330 node per iteration will not grow. This property ensures the scalability of the algorithm.

331 Substituting equation (7) into equation (5) yields the update equation of compensating α_j . Again,
 332 based on the converge-to-max criterion, we design the rate compensation iteration rule of random
 333 pairwise nodes. In this rule, the rate compensations of triggering node i , triggered node j , and silent
 334 nodes evolve as follows

$$\begin{cases} \alpha_j(t_{l+1}^{(ij)}) = \max\{\alpha_j(\tilde{t}_k^j), \alpha_{ji}(t_l^{(ij)})\alpha_i(t_l^{(ij)})\}, \\ \alpha_i(t_{l+1}^{(ij)}) = \max\{\alpha_i(\tilde{t}_k^i), \alpha_{ij}(t_l^{(ij)})\alpha_j(t_l^{(ij)})\}, \\ \alpha_{\text{silent}}(t_{l+1}^{(ij)}) = \alpha_{\text{silent}}(\tilde{t}_k^{\text{silent}}), \end{cases} \quad (8)$$

335 which means that random pairwise nodes i and j reach maximum logical clock together at a random
 336 gossip instant $t_{l+1}^{(ij)}$, and other nodes are silent. In equation (8), node i and j sequentially iterate its own
 337 estimated logical clock only once per gossiping interaction. Observing that whether \tilde{t}_k^i and \tilde{t}_k^j will be
 338 different or same depends on the contiguous activation of the Sync-L of global Poisson process.

339 After the rate compensation is applied, the random pairwise nodes compute the instantaneous
 340 estimated logical clock difference $T_i(t_l^{(ij)}) - T_j(t_l^{(ij)})$ and try to adjust its offset β in order to reduce the
 341 difference. Once again, the gossip consensus approach and the converge-to-max criterion are applied
 342 to local node i, j , and silent nodes for attaining offset compensations, as follows

$$\begin{cases} \beta_j(t_{l+1}^{(ij)}) = \beta_j(\tilde{t}_k^j) + \rho_2(T_i(t_l^{(ij)}) - T_j(t_l^{(ij)})), \\ \beta_i(t_{l+1}^{(ij)}) = \beta_i(\tilde{t}_k^i) + \rho_2(T_j(t_l^{(ij)}) - T_i(t_l^{(ij)})), \\ \beta_{\text{silent}}(t_{l+1}^{(ij)}) = \beta_{\text{silent}}(\tilde{t}_k^{\text{silent}}), \end{cases} \quad (9)$$

343 where $\rho_2 = 1$ and $T_i(t_l^{(ij)}) = \alpha_i(t_l^{(ij)})\tau_i(t_l^{(ij)}) + \beta_i(t_l^{(ij)})$. The flowchart of RGCS algorithm is shown in
 344 Figure 3(a), and the basic procedures are described as follows. Step 1. Randomly initialize each local
 345 clock τ_i . Step 2. Judge whether arbitrary node i activate its a neighbor or not, or is activated by its a
 346 neighbor or not. Step 3. Perform update equations (6), (7), (8), and (9). Step 4. Judge whether to meet
 347 the sync accuracy or not. Otherwise, return to Step 2.

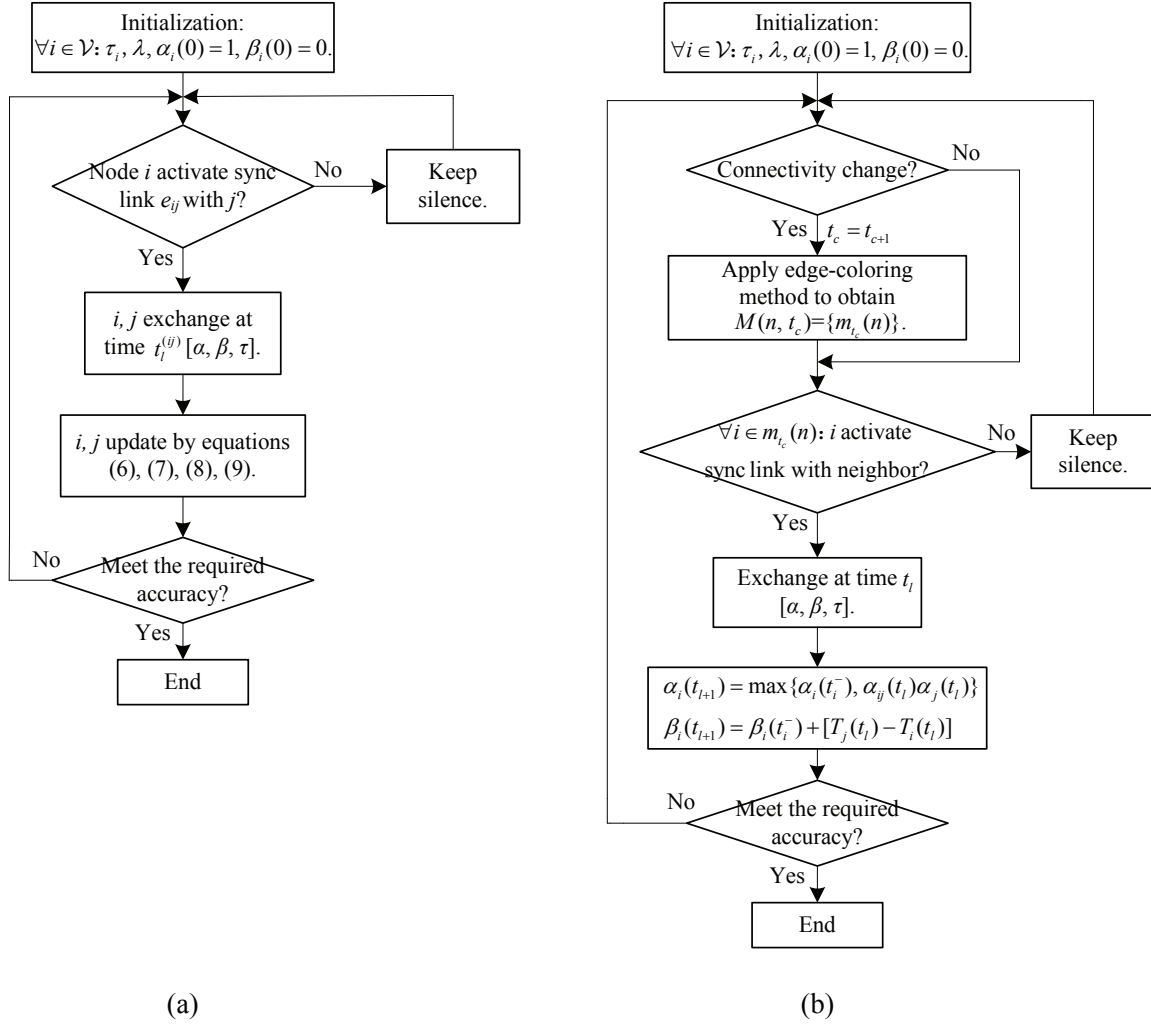


Figure 3. Flowchart of the proposed algorithms. (a) Randomized Gossip-Consensus-based time Synchronization (RGCS). (b) Multi-RGCS.

348 4.1.3. Convergence of RGCS

349 Substituting equation (2) into (3) yields an intuitive translation of the time synchronization issue:

$$\begin{cases} \Pr\{\lim_{t \rightarrow \infty} \tilde{\alpha}_i(t) = a_v\} = 1, \forall i \in \mathcal{V}, \\ \Pr\{\lim_{t \rightarrow \infty} \tilde{\beta}_i(t) = b_v\} = 1, \forall i \in \mathcal{V}, \\ \Pr[\tilde{\alpha}_i(t) - \tilde{\alpha}_j(t)] = o(1/t), \forall i, j \in \mathcal{V}, \end{cases} \quad (10)$$

350 where a_v and b_v are the parameters of consistent virtual clock. Equations (10) show that whether the
 351 clocks achieve synchronization or not depends not only on the convergence of logical rate and offset,
 352 but also on the convergence speed of the logical rate errors $\Pr[\tilde{\alpha}_i(t) - \tilde{\alpha}_j(t)]$, because errors will tend
 353 to diverge if the convergence speed to zero of $\Pr[\tilde{\alpha}_i(t) - \tilde{\alpha}_j(t)]$ is slower than $1/t$.

354 **Theorem 1.** Consider the rate and offset update equations given by Equation (6), (7), (8), (9), and
 355 there exist two variables $\Delta > 0$ and $l > 0$ such that the union graph $G(t_l^{(ij)}, \Delta(l, (ij))) = \cup_{ij} \cup_l \mathcal{G}(t_l^{(ij)})$
 356 for $\forall e_{ij} \in \mathcal{E}(t)$ is connected with probability one. Then, equations (10) hold true.

357 **Proof.** Firstly, two function $\mathcal{V}_v(t)$ and $|\mathcal{V}_v(t)|$ are introduced, where $\mathcal{V}_v(t)$ is the set of nodes whose
 358 logical rate and offset are equal to a_v and b_v in instant t , and $|\mathcal{V}_v(t)|$ is the cardinality of set $\mathcal{V}_v(t)$.

359 Define $a_{max} = \max\{a_i\}, \forall i \in \mathcal{V}$, let node v be the node whose clock rate is equal to a_{max} . According
 360 to the initial sets, there is at least one node in network whose logic clock rate and offset equal to a_v
 361 and b_v in initial instant, i.e., $\mathcal{V}_v(t) \neq \emptyset, |\mathcal{V}_v(t)| \geq 1$. With loss of generality, assume node j has larger
 362 logical rate. If the link e_{ij} is activated at gossip time $t_l^{(ij)}$, node i will update its logical clock such that
 363 $a_i\alpha_i = a_j\alpha_j, \alpha_i b_i + \beta_i = \alpha_j b_j + \beta_j$. Thus, the logical rate of each node is less than or equal to a_{max} during
 364 the iteration of RGCS. For a pair of nodes i and $j, i, j \in \mathcal{V}_v$, there has $a_i\alpha_i = a_{max}, \alpha_i b_i + \beta_i = \beta_v$ and
 365 $a_j\alpha_j = a_{max}, \alpha_j b_j + \beta_j = \beta_v$. Thus, we can infer that $a_i\alpha_i$ or $a_j\alpha_j \geq a_k\alpha_k$ holds for $\forall k \in \mathcal{V}$. Therefore,
 366 a pair of nodes i and j in \mathcal{V}_v will no longer update its logical clock and maintain its logical rate and
 367 offset during the latter iterations, which means that $|\mathcal{V}_v(t)|$ is nondecreasing.

368 The complement of a set \mathcal{V}_v is defined as $\mathcal{V} - \mathcal{V}_v$, which means that the set of nodes are not in \mathcal{V}_v .
 369 If node k is not in the set \mathcal{V}_v , then node k is in $\mathcal{V} - \mathcal{V}_v$. Since all nodes' logical rate is less than or equal
 370 to a_{max} during the iteration of RGCS, so we have $a_k\alpha_k < a_v$ for $\forall k \in \mathcal{V} - \mathcal{V}_v$. Thus, if node $i \in \mathcal{V}_v$ is
 371 coupled with node k by Sync-L, then it follows from equation (8) and (9) that node k will update its
 372 logical clock such that $a_k\alpha_k = a_v, \alpha_k b_k + \beta_k = \beta_v$. Then, one obtains that $|\mathcal{V}_v(t^+)| = |\mathcal{V}_v(t)| + 1$ and
 373 $|\mathcal{V} - \mathcal{V}_v(t^+)| = |\mathcal{V} - \mathcal{V}_v(t)| - 1$, where t^+ is the finish time of the iteration. Hence, $|\mathcal{V}_v(t)|$ will strictly
 374 increase when node $i \in \mathcal{V}_v$ is coupled with node $j \in \mathcal{V} - \mathcal{V}_v$.

375 If $|\mathcal{V}_v(t)| = N$ in instant t , it implies that $\Pr\{\lim_{t \rightarrow \infty} \tilde{\alpha}_i(t) = a^c\} = 1, \Pr\{\lim_{t \rightarrow \infty} \tilde{\beta}_i(t) = b^c\} = 1$,
 376 for $\forall i \in \mathcal{V}$. Otherwise, we have $|\mathcal{V}_v(t)| < N$. Since graph $G(t_l^{(ij)}, \Delta(l, (ij)))$ is jointly connected with
 377 probability one, there is at least one link e_{ik} for $i \in \mathcal{V}_v$ and $k \in \mathcal{V} - \mathcal{V}_v$, which means that there has
 378 $\lambda_{ik} > 0$. The probability of the event that link e_{ik} is activated satisfies $1 - e^{-\lambda_{ik}(t' - t)}$. Therefore, we
 379 have the probability of $|\mathcal{V}_v(t)| \geq |\mathcal{V}_v(t)| + 1$ being equal to $1 - e^{-\lambda_{ik}(t' - t)}$. Thus, $|\mathcal{V}_v(t)|$ will strictly
 380 increase with probability one when $t \rightarrow \infty$. Hence, we have $\Pr\{\lim_{t \rightarrow \infty} |\mathcal{V}_v(t)| = n\} = 1$ which yields
 381 $\Pr\{\lim_{t \rightarrow \infty} \tilde{\alpha}_i(t) = a^c\} = 1, \Pr\{\lim_{t \rightarrow \infty} \tilde{\beta}_i(t) = b^c\} = 1$, for $\forall i \in \mathcal{V}$. Then, $\Pr[a_i\alpha_i(t) - a_j\alpha_j(t)]$ can
 382 approximate to zero when $t \rightarrow \infty$. Clearly, $\lim_{t \rightarrow \infty} \Pr[a_i\alpha_i(t) - a_j\alpha_j(t)] / (1/t) = 0, \Pr[\tilde{\alpha}_i(t) - \tilde{\alpha}_j(t)] =$
 383 $o(1/t)$ thus satisfied. The Theorem 1 thus proved.

384 In practice, considering the thrift energy to bigger extent, finite-time convergence of algorithms
 385 is very important in WSNs. Next, we will give the lower bound of the probability for the finite-time
 386 convergence of RGCS. For node i, j , let's assume W_{ij} represents the time cost for a link activation event.
 387 Then $u_{ij}, U_{ij} = \int_0^t u_{ij}(s)ds$ is the probability density function and probability distribution function of
 388 W_{ij} , respectively.

389 **Theorem 2.** Suppose the union graph $G(t_l^{(ij)}, \Delta(l, (ij))) = \cup_{ij} \cup_l \mathcal{G}(t_l^{(ij)})$ for $\forall e_{ij} \in \mathcal{E}(t)$ is connected
 390 with probability one. Then, we have $\Pr\{T_i(t) = \tau_v(t), i \in \mathcal{V}\} \geq \prod_{i \in \mathcal{V}} U_{vi}(t)$.

391 **Proof.** From the proof of Theorem 1, we can conclude that node i in $\mathcal{V} - \mathcal{V}_v$ will become a node
 392 in \mathcal{V}_v after the link e_{vi} is activated. When $T_i(t) = \tau_v(t)$, there has $\Pr\{T_i(t) = \tau_v(t)\} = U_{vi}(t), i \in$
 393 \mathcal{V} . $\prod_{i \in \mathcal{V}} \Pr\{T_i(t) = \tau_v(t)\} \leq \Pr\{T_i(t) = \tau_v(t), i \in \mathcal{V}\}$ which yields $\Pr\{T_i(t) = \tau_v(t), i \in \mathcal{V}\} \geq$
 394 $\prod_{i \in \mathcal{V}} U_{vi}(t)$. The Theorem 2 thus proved.

395 4.2. Multi-RGCS Algorithm

396 Obviously, RGCS is obtained by the single-gossiping rule. Under this scenario, other silent nodes
 397 are situated in wait state, while only one synchronization link is activated in a timeslot. We expect that
 398 more coupling nodes are able to exchange and update states in a timeslot, or more than a neighboring
 399 node can overhear triggering node's messages (i.e. broadcast gossip manner). Based on their positive
 400 effect on the performance of the convergence rate, the Multi-gossiping version of RGCS (Multi-RGCS)
 401 is topic which is worth exploring. In fact, we can assume that more than two nodes (i, j, \dots) wake up in
 402 t_l simultaneously with probability $P(t_l) > 0$. So the single-gossiping version corresponds to specific
 403 implementation of above assumption in which if and only if two nodes i and j wake up.

404 Different from the foregoing single-gossiping, Multi-RGCS requires an additional precondition
 405 that the synchronization links can not have public vertex in the same slot. In other words, we need

406 to seek a multi-gossip sequence $M(n, t_c) = \{m_{t_c}(n)\}$, n is the color number, t_c is the switching time.
 407 So, the synchronization links are dyed different colors, and those links who have the same color are
 408 categorized as the group $m_{t_c}(n)$. This problem could be investigated by the idea of the Edge-Coloring
 409 (EC) [40]. The EC aims at an assignment of one color to each synchronization link such that no two
 410 synchronization links on the same node are assigned the same color. Here, we give a straightforward
 411 EC algorithm to realize Multi-RGCS as in Figure 3(b). Thereinto, the key procedures of obtaining the
 412 multi-gossip sequence are summarized as follows. For t_c do Step 1. Generate a spanning tree \mathcal{H}
 413 graph $\mathcal{G}(t_c)$; Step 2. Randomly pick a single edge in \mathcal{H} , find a non-adjacent edge to the former, find a
 414 nonstaining edge for coloring the third color, until it can not find any nonstaining edge. Step 3. The
 415 edges of different colors constitute the multi-gossip sequence $M(n, t_c) = \{m_{t_c}(1), m_{t_c}(2), \dots, m_{t_c}(n)\}$.
 416 The probability characteristics of the set $\{t_l, l = 1, 2, \dots\}$ is similar to the set $\{\cup_{l=0}^{\infty} \cup_{i=1, j=1}^N t_l^{(ij)}\}$, and
 417 the physical meaning of t_l^- refers to the previous gossip instant of any synchronization link involving
 418 node i . In Multi-RGCS, several nodes are involved in multi synchronization links $m_{t_c}(n)$ to increase
 419 the synchronization traffic and enhance the convergence speed.

420 4.3. Revised-RGCS Algorithm

421 In RGCS, we suppose that the delays is negligible. However, by considering various disturbance,
 422 which act as additive noise model (such as the delay), the actual timestamp is truly noisy, and the
 423 delay distribution is unknown. To deal with this issue, we proposed a least square estimation based
 424 low-pass filter against bounded delays (Assumption 2). As shown in Figure 4, the time-delay of the
 425 l th communication between node i and j is denoted by d_{ij} ($i \rightarrow j$, namely d_{ij} influences $\Delta S_j^{(ij)}$). d_{ij} is
 426 bounded by upper bound D ; that is, $0 < d_{ij} < D$. d_{ji} ($j \rightarrow i$, namely d_{ji} influences $\Delta S_i^{(ij)}$) is the same
 427 definition as d_{ij} , but may be unequal.

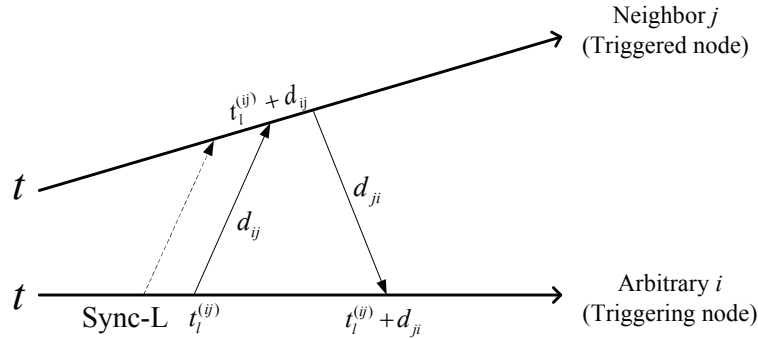


Figure 4. Illustration of gossip-consensus-based time synchronization with bounded delays.

428 Due to the symmetry, the following process takes the case of d_{ij} . Based on the definition of the
 429 relative drift and d_{ij} , we have a longspan estimator $\hat{\alpha}_{ij}(l)$ for $\alpha_{ij}(l)$ as follows

$$\begin{aligned}
 \hat{\alpha}_{ij}(l) &= \frac{\tau_j(t_l^{(ij)} + d_{ij}(l)) - \tau_j(t_0^{(ij)} + d_{ij}(0))}{\tau_i(t_l^{(ij)}) - \tau_i(t_0^{(ij)})} \\
 &= \frac{a_j(\sum^l \delta_{ij}(l) + d_{ij}(l) - d_{ij}(0))}{a_i \sum^l \delta_{ij}} \\
 &= \alpha_{ij}(1 + \hat{\xi}(l)), \tag{11}
 \end{aligned}$$

430 where $\hat{\xi}(l) = \frac{d_{ij}(l) - d_{ij}(0)}{\sum^l \delta_{ij}}$, δ_{ij} is the inter-time between consecutive gossip instants for link e_{ij} . Since d_{ij}
 431 is bounded by D , we have $|\hat{\xi}(l)| \leq \frac{D}{\sum^l \delta_{ij}}$. Hence, we know $\hat{\xi}(l)$ decays in a rate of $\mathcal{O}(1/\delta)$.

432 Let $\hat{\alpha}_{ij}^*(l)$ be the optimal estimator for $\hat{\alpha}_{ij}(l)$, and denote $e_l = \hat{\alpha}_{ij}(l)\tau_i(t_l^{(ij)}) - \hat{\alpha}_{ij}^*(l)\tau_i(t_l^{(ij)})$. A least
 433 square principle as $J = \sum_{l=1}^L e_l^2$ is employed. For calculating the recursion of $\hat{\alpha}_{ij}^*(l)$, we apply a partial
 434 derivative for $\hat{\alpha}_{ij}^*(l)$, namely

$$\frac{\partial J}{\partial \hat{\alpha}_{ij}^*(l)} = 0, \quad (12)$$

435 which yields a optimal estimator as follow

$$\hat{\alpha}_{ij}^*(l) = (1 - \gamma^*(l))\hat{\alpha}_{ij}^*(l-1) + \gamma^*(l) \frac{\tau_j(t_l^{(ij)}) - \tau_j(t_0^{(ij)})}{\tau_i(t_l^{(ij)}) - \tau_i(t_0^{(ij)})}, \quad (13)$$

436 where the weighting parameter $\gamma^*(l) = \frac{\delta^2(1)+\delta^2(2)+\dots+\delta^2(l)}{\delta^2(1)+(\delta^2(1)+\delta^2(2))+\dots+(\delta^2(1)+\delta^2(2)+\dots+\delta^2(l))}$ and $\hat{\alpha}_{ij}^*(0) = 1$.
 437 Substituting equation (11) into (13) yields

$$\hat{\alpha}_{ij}^*(l) = \alpha_{ij}(1 + \hat{\xi}^*(l)), \quad (14)$$

438 where $\hat{\xi}^*(l) = \frac{\delta(1)+(\delta(1)+\delta(2))+\dots+(\delta(1)+\delta(2)+\dots+\delta(l))(d_{ij}(l)-d_{ij}(0))}{\delta(1)+(\delta(1)+\delta(2))^2+\dots+(\delta(1)+\delta(2)+\dots+\delta(l))^2}$. Then by bounded d_{ij} , and we notice
 439 that, the denominator of $\hat{\xi}^*(l)$ is δ 's quadratic term after accumulating, and the numerator of $\hat{\xi}^*(l)$ is
 440 δ 's first degree term. It implies that the decay rate of $\hat{\xi}^*(l)$ is also $\mathcal{O}(1/\delta)$. This decay rate ensures
 441 that the proposed least square estimation based low-pass filter avoids the divergence condition of
 442 $\Pr[\tilde{\alpha}_i(t) - \tilde{\alpha}_j(t)]$. Hence, we can utilize $\frac{\hat{\alpha}_{ij}^*(l)}{(\delta(1)+\delta(1)+\delta(2)+\dots+\delta(l))^{1/2}}$ to replace $\alpha_{ij}(t_l^{ij})$ and modify the rate
 443 updating rule of triggering node i of equations (6), there is

$$\alpha_i(t_{l+1}^{(ij)}) = \left(1 - \frac{\rho_1}{(\delta(1) + \delta(1) + \delta(2) + \dots + \delta(l))^{1/2}}\right) \alpha_i(\tilde{t}_k^i) + \frac{\rho_1 \hat{\alpha}_{ij}^*(l) \alpha_j(t_l^{(ij)})}{(\delta(1) + \delta(1) + \delta(2) + \dots + \delta(l))^{1/2}}. \quad (15)$$

444 The criterion for selecting the appropriate weighting parameter $(\delta(1) + \delta(1) + \delta(2) + \dots + \delta(l))^{-1/2}$ is
 445 based on a piece-wise constant function, and it is chosen to be a decreasing factor, which contributes to
 446 restraining the negative effect of additive noise in stochastic approximation. Actually, the weighting
 447 parameter in this paper is a special case of the standard conditions in stochastic approximation
 448 methods: $\sum_{l=1}^{\infty} (\delta(1) + \delta(1) + \delta(2) + \dots + \delta(l))^{-1/2} = \infty$ and $\sum_{l=1}^{\infty} (\delta(1) + \delta(1) + \delta(2) + \dots + \delta(l))^{-1} < \infty$.
 449 Since $\alpha_{ij}(t_l^{(ij)})$ is an estimation of inverse relative drift $\alpha_{ji}(t_l^{(ij)})$, the rate updating rule of triggered
 450 node j is

$$\alpha_j(t_{l+1}^{(ij)}) = \left(1 - \frac{1 - \rho_1}{(\delta(1) + \delta(1) + \delta(2) + \dots + \delta(l))^{1/2}}\right) \alpha_j(\tilde{t}_k^j) + \frac{(1 - \rho_1) \alpha_i(t_l^{(ij)})}{\hat{\alpha}_{ij}^*(l) (\delta(1) + \delta(1) + \delta(2) + \dots + \delta(l))^{1/2}}. \quad (16)$$

451 Then, the clock offset compensations of local node i, j is updated as follows

$$\beta_i(t_{l+1}^{(ij)}) = \beta_i(\tilde{t}_k^i) + \rho_2 (T_j(t_l^{(ij)}) - T_i(t_l^{(ij)}) + d_{ji}(l)). \quad (17)$$

$$\beta_j(t_{l+1}^{(ij)}) = \beta_j(\tilde{t}_k^j) + \rho_2 (T_i(t_l^{(ij)}) - T_j(t_l^{(ij)}) + d_{ij}(l)). \quad (18)$$

452 The delays also have impact on \tilde{t}_k^i . The issue is caused by the fact that node j would not instantly
 453 receive its gossiping neighbor's states due to uncertain delay, and if delay d_{ij} satisfy following two
 454 conditions: (i) delay d_{ij} greater than inter-time Δ ; (ii) node j joins next gossip averaging; \tilde{t}_k^i will change
 455 and need to be modified. When $d_{(ij)} \neq d_{(ji)}$, we call asymmetric gossip, and that is a common case.

456 To clearly explain how delay influence the local updating equations, we might as well suppose link
 457 e_{ij} is activating. After Δ , there are three possibilities of adjacent Sync-L: $e_{ik}, e_{jh}, e_{kh}, \forall k, h \in \mathcal{V}$, if:

458 Case 1, $d_{ij} \geq \Delta(l, (ik)) + n\Delta(l, (kh)), n = 0, 1, \dots$, then equations (16), (18) utilize $\hat{\alpha}_{ik}^*(l)$ and $\tilde{t}_k^i =$
 459 $\max\{t_s^{(ik)}, t_r^{(ki)} | s, r = 1, 2, \dots\}$. Case 2, $d_{ji} \geq \Delta(l, (jh)) + n\Delta(l, (kh)), n = 0, 1, \dots$, then equations (15),
 460 (17) utilize $\hat{\alpha}_{jh}^*(l)$ and $\tilde{t}_h^j = \max\{t_s^{(jh)}, t_r^{(hj)} | s, r = 1, 2, \dots\}$.

461 The discriminant of Case 1 and Case 2 is easy to implement, because the comparison between
 462 the length of delay and the interval time of node activation depends on the local nodes themselves.
 463 The delays make Revised-RGCS slightly complex, but it will not damage the convergence. However,
 464 we should point out that the update of the logical rate is based on the longspan neighboring states
 465 $\tau_j(t_l^{(ij)}) - \tau_j(t_0^{(ij)})$, so the nodes should set up a cached memory for forming buffer queue of the timing
 466 messages. Summarize the above process, a flow diagram of the Revised-RGCS algorithm is described
 467 in Figure 5.

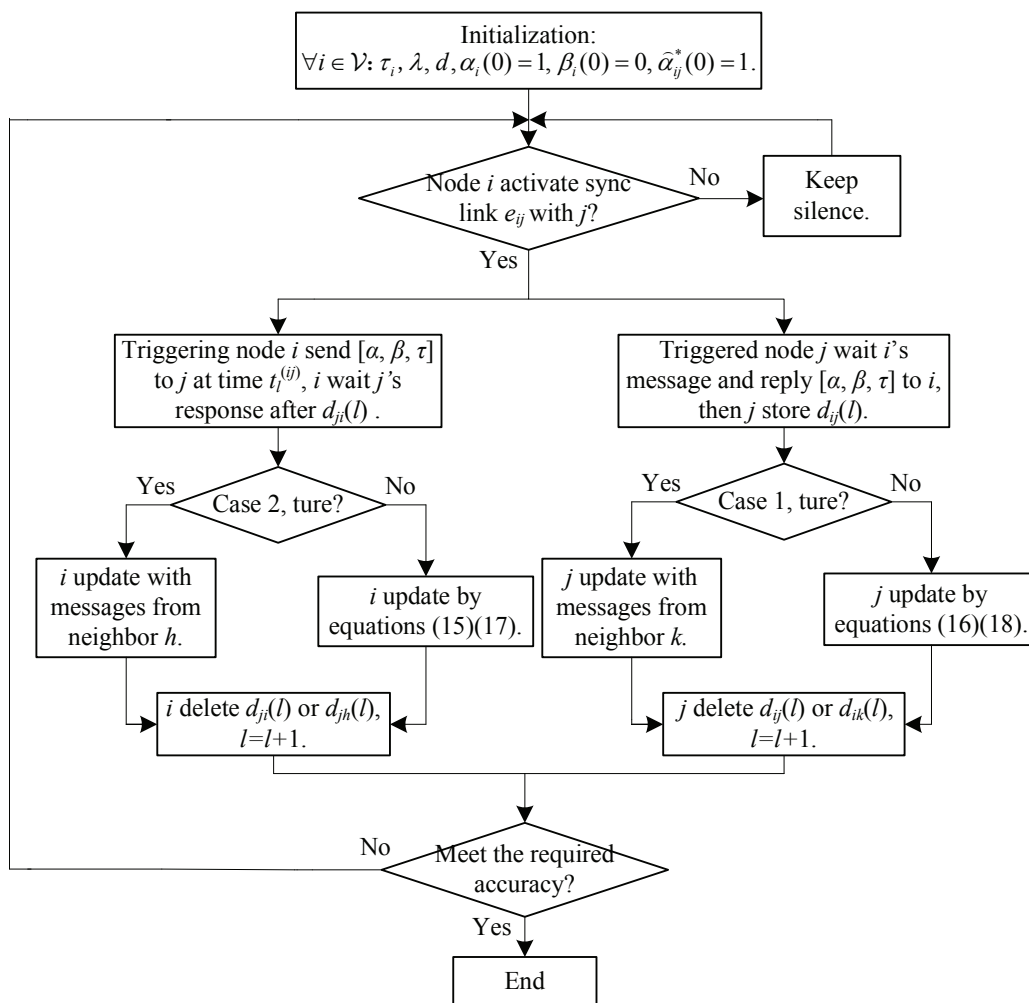


Figure 5. Flowchart of Revised-RGCS algorithm.

468 5. Simulation Studies

469 To verify the superiority of novel proposed algorithms, we carried out comparative simulations
 470 for RGCS and Multi-RGCS with delay-free case in the Matlab R2010b. Then, using the OMNeT++ 5.1
 471 simulator, a more realistic simulator for WSNs, we verified the Revised-RGCS algorithm with delays.

472 5.1. Delay-Free Case

473 As shown in Table 1, DCS and RPCS are two appropriate reference algorithms, so we compared
 474 the performances of RGCS with them. All of them have been investigated numerically for emulating a
 475 randomly connected ad hoc WSN. The important parameter setting is described as follows. The local
 476 hardware rate is chosen from $[0.999, 1.0001]$, and the local offset is chosen from $[0, 0.002]$. $\alpha_i(0) = 1$
 477 and $\beta_i(0) = 0$. The number of nodes is 9, and the number of local nodes that can be accessed by
 478 other nodes is 3. The initial synchronization period is 10 s. The threshold of successful Sync-L is
 479 characterize by a Poisson process with intensity λ , and the intensity reflects the connection strength
 480 between individual nodes. The average number of Sync-L per time interval is 10. It is feasible that
 481 the joint topologies of simulation model of dynamic WSN are connected with probability one. The
 482 time unit is one second. The required accuracy is ± 1 millisecond. Because there are no reference
 483 nodes and random initial parameters, we employed a metric to evaluate the synchronization error of
 484 the algorithms: the maximum difference of the parameters between any two nodes in overall WSN
 485 [18–20], i.e. $\eta_{95\%}(t) \geq 95\%$, where $\eta(t) = \frac{\max_{i,j} |X_i(0) - X_j(0)| - \max_{i,j} |X_i(t) - X_j(t)|}{\max_{i,j} |X_i(0) - X_j(0)|} \cdot 100\%$, for $\forall i, j \in \mathcal{V}$.

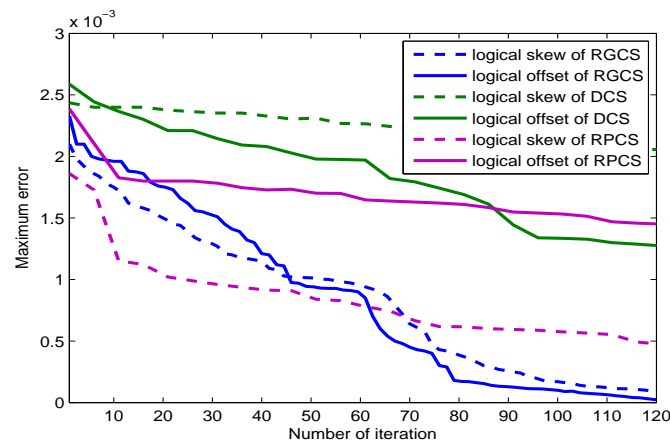


Figure 6. Comparison of maximum error of rate $\tilde{\alpha}_i(t)$ and offset $\tilde{\beta}_i(t)$ between RGCS algorithm and the reference algorithms.

486 Figure 6 shows the maximum error of logical rate $\tilde{\alpha}_i(t)$ and offset $\tilde{\beta}_i(t)$ under RGCS and DCS.
 487 In our algorithm, logical rate and offset synchronization can be achieved simultaneously. So, RGCS
 488 designed for randomly connected WSNs is an asynchronous and distributed configuration, and can
 489 make a complete compensation for the rate and offset. Due to the dense node density, DCS can not
 490 achieve rate compensation and offset compensation simultaneously. Because DCS devised for sparse
 491 node density to tolerate long delays leads to the synchronous mode for the update of the rate and
 492 offset. At the beginning of the compensation in RPCS, the rate of the rate compensation is faster than
 493 that in RGCS, because RPCS employs a standard frequency estimation technique to obtain an estimate
 494 of the pairwise drift. However, the descending rate of the offset compensation is relative slow, and
 495 the logical clock $T_i(t)$ could not be synchronized without the backward jumps phenomenon.

496 Figure 7 shows the maximum error of $T_i(t)$ of RGCS under $\lambda = 1, 5, 10$, from which it can be
 497 observed that it takes less time with $\lambda = 10$ to reach synchronization. This is because a larger intensity
 498 of Poisson process can decrease inter-time $\Delta(l, (ij))$ between consecutive gossip instants for any links.
 499 The results in Figure 6 validate the theoretical features of equation (3). So the descent velocity of the
 500 maximum error of logical clocks with $\lambda = 10$ becomes more remarkable.

501 Figure 8 shows the comparative simulation results with regard to single RGCS and Multi-RGCS.
 502 The green line represents the convergence of logical clocks in Multi RGCS. Falling speed of green line
 503 is faster than blue line (single RGCS), because more clocks exchange their states and come close to

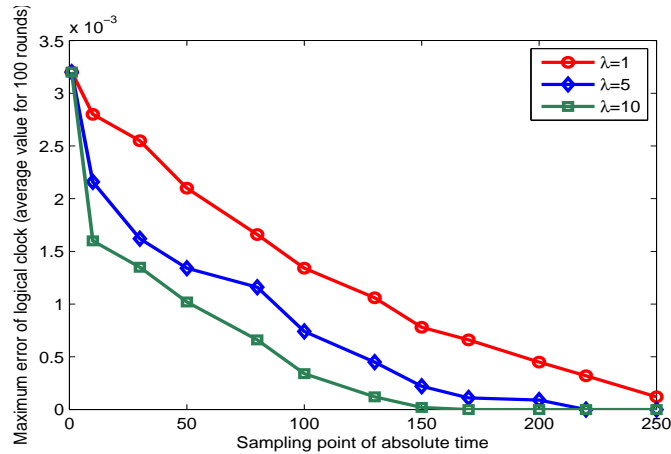


Figure 7. Comparison of maximum errors of logical clocks $T_i(t)$ of RGCS under different λ (the same initialization values of clocks for comparing intuitively).

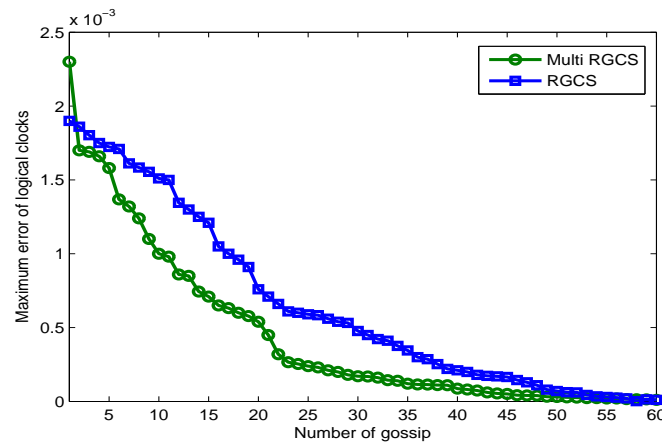


Figure 8. Comparison of maximum errors of $T_i(t)$ between single RGCS and Multi-RGCS.

504 the maximum-value at each gossip instant. Then, Figure 9 shows the relationship between different
 505 coloring edge's number ranging from $n = 5$ to $n = 12$ and 95th percentile of synchronization errors.
 506 The performance degrades as more coloring number increase, however it exhibits a approximative
 507 linear dependence, thus it refers to the amount of gossip as a function of the coloring number n . So
 508 we can involve this feature to suppress drift for different synchronization accuracies.

509 Based on the above simulation results and discussions, it can be seen that the paper has proposed
 510 a RGCS algorithm with superior performances compared to existing methods in term of dynamic
 511 adaptability and faster convergence speed. A edge-coloring algorithm can be applied to constitute a
 512 spanning tree so that Multi RGCS has faster convergence speed than that in RGCS.

513 5.2. Bounded Delay Case

514 OMNeT++ is an extensible, modular, component-based C++ simulation library and framework,
 515 primarily for building network simulators. Based on MiXiM framework and Network Description
 516 (NED) files, we implement an ad hoc WSN on the OMNeT++ 5.1.1, and then run the Revised-RGCS
 517 algorithm on it. It has been simulated for WSNs of $N = 9$ clocks placed on a field of size $100\text{m} \times 100\text{m}$.
 518 Moving sensors indexed by bidimensional coordinate XY, namely node11, node12, node13, node21,
 519 node22, node23, node31, node32 and node33. For those mobile nodes, we used the Random Walk
 520 module to locate the coordinate position of the node. In this module, each node was made to move

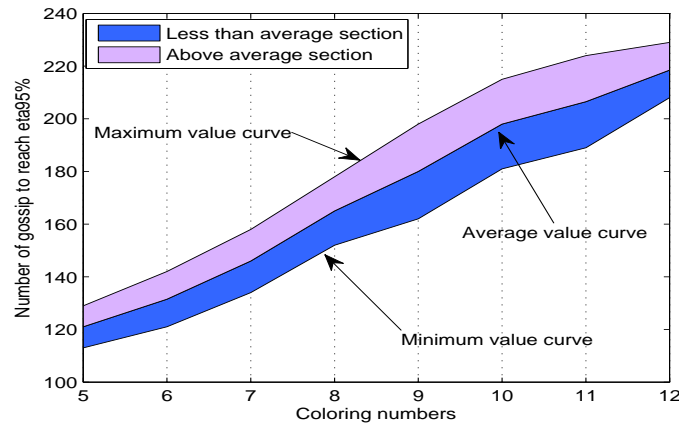


Figure 9. The relationship between the number of gossip and coloring number (simulate it for 10).

521 to next coordinate position at random. Note that the radios in a node could collect incident message
 522 sets with higher layer module operation decoupled by buffers, so deferred message will be valid.
 523 Summarize the key parameters into Table 2.

Table 2. Simulation Parameters

Module	Parameter and Data Value
Application	250 kbps data rate
Wireless channel	Bandwidth: 20 MHz, Data rate: 250 kbps Modulation type: BPSK
Radio	Sensitivity: -95 dBm, Noise floor: -100 dBm, Transmit power: 0 dBm, Mode: Ideal
Tunable MAC	Timestamp and default parameters
Communication radius	10m, 20m, 30m for every three nodes
Mobility model	Random walk (mobility update interval = 100 ms, speed = 5 m/sec)
Initial energy	28080 J
Field size	100m×100m
Simulation time	600 secs

524 The probability density distributions of time-delays d_{ij} and d_{ji} are shown in Figure 10. We carried
 525 on the statistics from 10 times simulations and obtain the distribution of them. It can be seen that
 526 the maximum delay is bounded which confirms the realistic bounded model. In reality, d_{ij} is often
 527 different from d_{ji} because the uplink and downlink between head and tail are independent of one
 528 another. Obviously, Revised-RGCS is an asymmetric gossip. In RPCS, the authors assume reciprocal
 529 propagation delays $d_{ij} = d_{ji}$ in each synchronization round. The delay assumption in this paper is
 530 more practical than that in the RPCS.

531 With the bounded delays, we compared the relative drift estimation method, which is based on
 532 low-pass filter, used in Revised-RGCS and that in RGCS. Figure 11 shows the results of relative drift
 533 estimation error $\hat{\xi}^*(l)$ of random pairwise nodes. It is observed that using equation (14), relative drift
 534 α_{ij} can be estimated accurately as $\hat{\alpha}_{ij}^*(l)$ (the blue line) will converge to the ideal value. Oppositely,
 535 the average estimate error is diverging in RGCS (the green line) without the low-pass filter. We see that
 536 the relative rate estimation under the bound delay can be obtained with Revised-RGCS, on which an
 537 effective timing protocol depends.

538 The simulation results of the Revised-RGCS, DCS and RPCS implementations are presented in
 539 Figure 12. It is observed from Figure 12 that Revised-RGCS takes about 20 synchronization rounds to
 540 reach within 10 ticks while RPCS does not achieve the expected error before 20 rounds. It is clear that

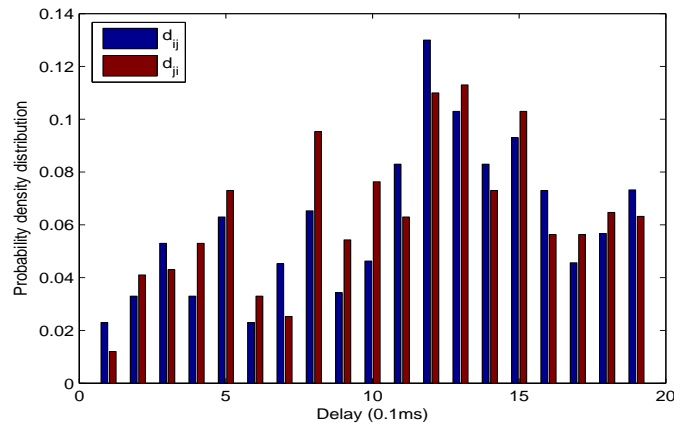


Figure 10. The difference of d_{ij} and d_{ji} .

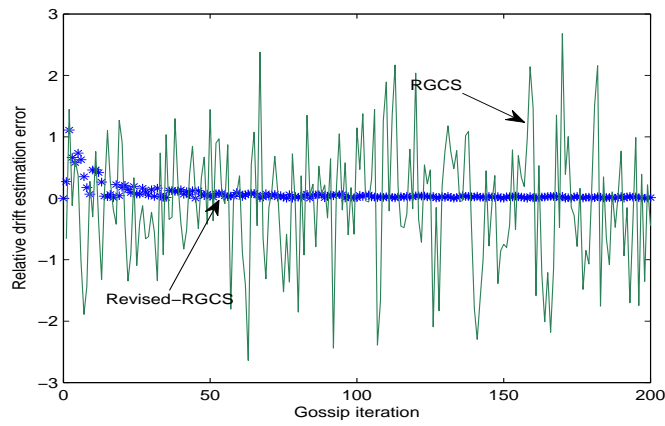


Figure 11. Comparison of relative drift estimation error between Revised-RGCS and RGCS.

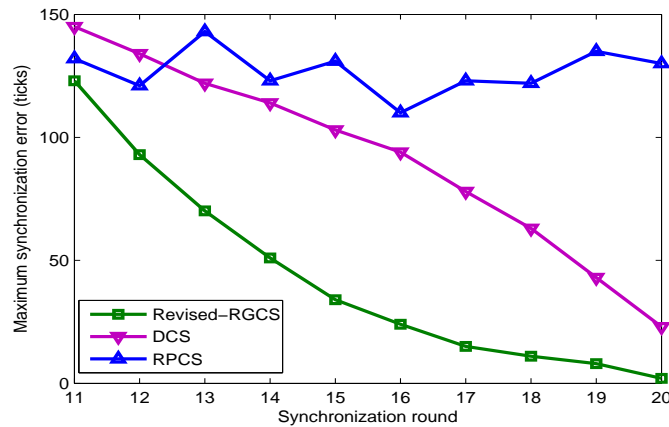


Figure 12. Comparison of maximum synchronization error (ticks) between Revised-RGCS algorithm and the current algorithms.

541 the Revised-RGCS can ensure that the sync error is bounded. In contrast, due to symmetric delay,
 542 the maximum synchronization error of the RPCS is ceaselessly growing. The results demonstrate that
 543 Revised-RGCS converges asymptotically while RPCS is diverging. Although the DCS algorithm can

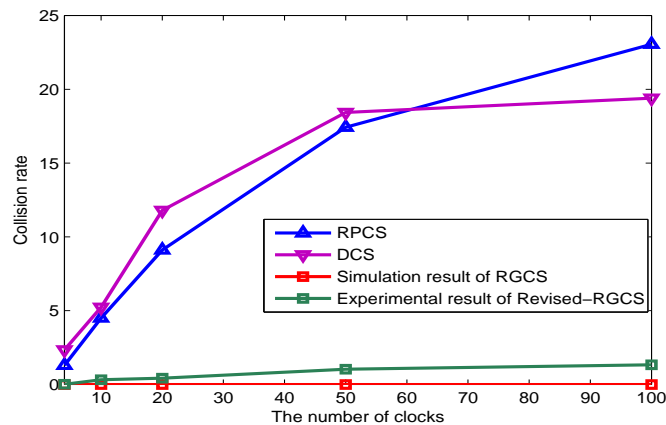


Figure 13. Comparison of Revised-RGCS, RGCS, DCS, and RPCS on collision rate as the number of clocks increasing.

544 reach time synchronization, but its convergence rate is relatively slow under the randomly connected
 545 scene. This is because in DCS, the offset and rate compensation are initiated by the updated table
 546 information which is a weighted averages of the neighborhoods.

547 Most of the existing timing protocols employ a deterministic periodic synchronization scheme
 548 which results in message collisions, and they focus concentrate on which merely exploit a packet in
 549 a collision timeslot or directly discard redundant packets. These techniques are passive to a certain
 550 extent. The reason for this is that WSNs require a nontrivial collision detection scheme and invalid
 551 packets waste energy. In RGCS, we assume that every gossiping of a pair of nodes costs the same
 552 amount of energy E_{eg} and let E_g be the total energy cost for gossiping to the expected accuracy, then
 553 $E_s = E_g = \sum_{l=1, e_{ij}}^N \delta(l, (ij)) \times E_{eg}$ for $\forall e_{ij} \in \mathcal{E}(t)$. As discussed in the Section 2, we know that, in most
 554 of distributed configuration protocols, the similar hardware clock states is the main reason behind the
 555 message collisions of hidden nodes. Hence, the number of clocks is considered to be an evaluation
 556 indicator. Figure 13 shows the timing message collision rate versus the number of clocks. The timing
 557 collision rate of RPCS and DCS protocols achieve 23.4%, 19.2% when the network scale is 100. In
 558 simulation, due to asynchronous pairwise policy and an appropriate λ , the collision rate of RGCS is
 559 null. In the Revised-RGCS, the collision rate is 2.1%, because the timing messages are delivered to the
 560 MAC layer of the nodes with long delays which collides with the Sync-L event at few instants.

561 Based on the above simulation results and discussions, the Revised-RGCS can guarantee time
 562 synchronization under realistic bounded delay model with low collision rate compared to the current
 563 algorithms in practice.

564 6. Conclusions

565 This paper presents a new randomized and energy-efficient time synchronization protocol called
 566 RGCS for dynamic WSNs with randomly changing connectivity. The protocol is based on distributed
 567 consensus timesync but incorporating with the gossip algorithm. Therefore, it is superior to existing
 568 protocols in a generalized randomization framework, and can be well adapted to the link variation
 569 of ad hoc WSNs dynamically. The new idea of randomized scheduling of the synchronization links
 570 is to lower the rate of collision, so the RGCS dramatically relieves the collisions phenomenon. Based
 571 on the converge-to-max criterion, the method has been deduced to accelerate the convergence speed.
 572 By combining the idea of the EC, Multi-RGCS has been proposed. Moreover, Revised-RGCS has been
 573 developed to specially restrain the impact of uncertain bounded delays. Extensive simulations have
 574 demonstrated the better performances of the proposed protocols.

575 The proposed EC method is rough, since the dynamic ad hoc WSNs need a global coordinator in
 576 order to produce a spanning tree at each changing moment of topology. It is worth investigating how
 577 to design pure distributed EC algorithm for Multi-RGCS. This will enhance the adaptability for fast
 578 changing networks. However, pure distributed edge-coloring is to be NP-Complete. In future work,
 579 we will focus on developing a solution to find the maximum clique of the sync edges.

580 **Acknowledgments:** This work was supported by the National Natural Science Foundation of China under grant
 581 No. 61633016.

582 **Author Contributions:** Nan Xiong and Minrui Fei made substantial contributions to the original ideas on RGCS,
 583 Multi RGCS, and Revised-RGCS. Nan Xiong carried out the simulations and wrote the paper. Taicheng Yang
 584 provided critical guidance and given quite a lot of suggestions during the research and paper revising.

585 **Conflicts of Interest:** The authors declare that there are no conflicts of interest.

586 Bibliography

- 587 1. Wu, F.-J.; Kao, Y.-F.; Tseng, Y.-C. From wireless sensor networks towards cyber physical systems. *Pervasive*
 588 *Mob. Comput.* **2011**, *7*, 397-413.
- 589 2. Mahmood, A.; Exel, R.; Trsek, H.; Sauter, T. Clock synchronization over IEEE 802.11 - a survey of
 590 methodologies and protocols. *IEEE Trans. Ind. Inf.* **2017**, *13*, 907-922.
- 591 3. Zhang, R.-H.; He, Z.-C.; Wang, H.-W.; et al. Study on self-tuning tyre friction control for developing
 592 main-servo loop integrated chassis control system. *IEEE Access* **2017**, *5*, 6649-6660.
- 593 4. Huang, P.-H.; Maulik, D.; Qiu, X.F.; et al. On the multihop performance of synchronization mechanisms in
 594 high propagation delay networks. *IEEE Trans. Comput.* **2009**, *58*, 577-590.
- 595 5. Du, J.; Wu, Y.-C. Distributed clock skew and offset estimation in wireless sensor networks: Asynchronous
 596 algorithm and convergence analysis, *IEEE Trans. Wirel. Commun.* **2013**, *12*, 5908-5917.
- 597 6. Yildirim, K.-S.; Kantarci, A. Time synchronization based on slow-flooding in wireless sensor networks,
 598 *IEEE Trans. Parallel Distrib. Syst.* **2014**, *25*, 244-253.
- 599 7. Cao, X.-Y.; Yang, F.; Gan, X.-Y.; Liu, J.; et al. Joint estimation of clock skew and offset in pairwise broadcast
 600 synchronization mechanism. *IEEE Trans. Commun.* **2013**, *61*, 2508-2521.
- 601 8. Ren, F.-Y.; Lin, C.; Liu, F. Self-correcting time synchronization using reference broadcast in wireless sensor
 602 network. *IEEE Wirel. Commun.* **2008**, *15*, 79-85.
- 603 9. Meng, Y.; Li, T.; Zhang, J.-F. Finite-level quantized synchronization of discrete-time linear multi-agent
 604 systems with switching topologies. *SIAM J. Control Optim.* **2017**, *55*, 275-299.
- 605 10. Zong, X.-F.; Li, T.; Zhang, J.-F. Consensus conditions of continuous-time multi-agent systems with additive
 606 and multiplicative measurement noises. *SIAM J. Control Optim.* **2018**, *56*, 19-52.
- 607 11. Schenato, L.; Fiorentin, F. Average TimeSynch: A consensus-based protocol for clock synchronization in
 608 wireless sensor networks. *Automatica* **2011**, *47*, 1878-1886.
- 609 12. He, J.-P.; Cheng, P.; Shi, L.; Chen, J.-M. Time synchronization in WSNs: A maximum-value-based consensus
 610 approach. *IEEE Trans. Autom. Control* **2014**, *59*, 660-675.
- 611 13. Panigrahi, N.; Khilar, P. M. An evolutionary based topological optimization strategy for consensus based
 612 clock synchronization protocols in wireless sensor network. *Swarm Evol. Comput.* **2015**, *22*, 66-85.
- 613 14. Saiah, A.; Benzaid, C.; Badache, N. CMTS: Consensus-based multi-hop time synchronization protocol
 614 in wireless sensor networks. In Proceedings of the IEEE 15th International Symposium on Network
 615 Computing and Applications, Cambridge, United States, October 30, 2016 - November 2, 2016; pp. 232-236.
- 616 15. Garone, E.; Gasparri, A.; Lamonaca, F. Clock synchronization protocol for wireless sensor networks with
 617 bounded communication delays. *Automatica* **2015**, *59*, 60-72.
- 618 16. Tian, Y.-P. LSTS: A new time synchronization protocol for networks with random communication delays. In
 619 Proceedings of the 2015 IEEE 54th Annual Conference on Decision and Control Conference, Osaka, Japan,
 620 15-18 December 2015; pp.7404-7409.
- 621 17. Tian, Y.-P.; Zong, S.-H.; Cao, Q.-Q. Structural modeling and convergence analysis of consensus-based time
 622 synchronization algorithms over networks: Non-topological conditions. *Automatica* **2016**, *65*, 60-75.

- 623 18. Lamonaca, F.; Gasparri, A.; Garone, E.; Grimaldi, D. Clock synchronization in wireless sensor network with
624 selective convergence rate for event driven measurement applications. *IEEE Trans. Instrum. Meas.* **2014**, *63*,
625 2279-2287.
- 626 19. Brown, D. R.; Klein, A. G.; Wang, R. Monotonic mean-squared convergence conditions for random pairwise
627 consensus synchronization in wireless networks. *IEEE Trans. Signal Process* **2015**, *63*, 988–1000.
- 628 20. Sun, W.-L.; Strom, E.G.; Brannstrom, F.; Gholami, M.R. Random broadcast based distributed consensus
629 clock synchronization for mobile networks. *IEEE Trans. Wireless Commun.* **2015**, *14*, 3378-3389.
- 630 21. Bolognani, S.; Carli, R.; Lovisari, E.; Zampieri, S. A randomized linear algorithm for clock synchronization
631 in multi-agent systems. *IEEE Trans. on Autom. Control* **2016**, *61*, 1711-1726.
- 632 22. He, J.-P.; Cheng, P.; Shi, L.; et al. SATS: Secure average-consensus-based time synchronization in wireless
633 sensor networks. *IEEE Transaction on Signal Processing* **2013**, *61*, 6387-6400.
- 634 23. Dong, W.; Liu, X.-J. Robust and secure time-synchronization against sybil attacks for sensor networks. *IEEE*
635 *Transactions on Industrial Informatics* **2015**, *11*, 1482-1491.
- 636 24. Katarzyna, K.-S. A survey of MAC layer solutions to the hidden node problem in ad-hoc networks. *Ad Hoc*
637 *Networks* **2012**, *10*, 635-660.
- 638 25. Boyd, S.; Ghosh, A.; Prabhakar, B.; Shah, D. Randomized gossip algorithms. *IEEE Trans. Inf. Theory* **2006**,
639 *52*, 2508-2530.
- 640 26. Dimakis, A.G.; Kar, S.; Moura, J.M.F.; et al. Gossip algorithms for distributed signal processing. *Proceedings*
641 *of the IEEE* **2010**, *98*, 1847-1864.
- 642 27. Lavaei, J.; Murray, R. M. Quantized consensus by means of gossip algorithm. *IEEE Trans. on Autom. Control*
643 **2012**, *57*, 19-32.
- 644 28. Picci, G.; Taylor, T.-J. Almost sure exponential convergence to consensus of random gossip algorithms, *Int.*
645 *J. Robust Nonlinear Control* **2013**, *23*, 1033–1045.
- 646 29. Franceschelli, M.; Giua, A.; Seatzu, C. Fast discrete consensus based on gossip for makespan minimization
647 in networked systems. *Automatica* **2015**, *56*, 60-69.
- 648 30. Du, J.; Wu, Y.-C. Distributed clock skew and offset estimation in wireless sensor networks: Asynchronous
649 algorithm and convergence analysis, *IEEE Trans. Wireless Commun.* **2013**, *12*, 5908–5917.
- 650 31. Choi, B. J.; Liang, H.; Shen, X.; Zhuang, W.-H. DCS: distributed asynchronous clock synchronization in
651 delay tolerant networks. *IEEE Trans. Parallel Distrib. Syst.* **2012**, *23*, 491–504.
- 652 32. Ahmed, S.; Xiao, F.; Chen, T.-W. Asynchronous consensus-based time synchronisation in wireless sensor
653 networks using unreliable communication links. *IET Control Theory Appl.* **2014**, *8*, 1083–1090.
- 654 33. Huang, G.; Zomaya, A. Y.; Delicato, F. C.; Pires, P.F. An accurate on-demand time synchronization protocol
655 for wireless sensor networks. *J. Parallel Distrib. Comput.* **2012**, *72*, 1332–1346.
- 656 34. Nicolas, M.; Jean-Benoit, P.; Jean-Marie, G. Fine synchronization for wireless sensor networks using gossip
657 averaging algorithms. In Proceedings of the 2008 IEEE International Conference on Communications,
658 Beijing, China, 19-23 May 2008; pp.4963-4967.
- 659 35. Saverio, B.; Ruggero, C.; Sandro, Z. A PI consensus controller with gossip communication for clock
660 synchronization in wireless sensors networks. In Proceedings of the 1st IFAC Workshop on Estimation
661 and Control of Networked Systems, Venice, Italy, 24-26 September 2009; pp.78-83.
- 662 36. Baldoni, R.; Corsaro, A.; Querzoni, L.; Scipioni, S.; Tucci Piergiovanni, S. Coupling-based internal clock
663 synchronization for large-scale dynamic distributed systems. *IEEE Trans. Parallel Distrib. Syst.* **2010**, *21*,
664 607–619.
- 665 37. Joerg, S.; Patrick, J.; Reinhold, H-U. A gossiping approach to sampling clock synchronization in wireless
666 acoustic sensor networks. In Proceedings of the 2014 IEEE International Conference on Acoustics, Speech,
667 and Signal Processing, Florence, Italy, 4-9 May 2014; pp.7575-7579.
- 668 38. Stankovic, M.S.; Stankovic, S.S.; Johansson, K.H. Asynchronous distributed blind calibration of sensor
669 networks under noisy measurements. *IEEE Trans. Control Netw. Syst.* **2018**, *5*, 571-582.
- 670 39. Zhang, D.-S.; Tian, H.; Liu, Y.-H.; et al. Poster: Neighbor discovery with distributed quorum system. In
671 Proceedings of the 9th ACM Conference on Embedded Networked Sensor Systems, Seattle, United States,
672 1-4 November 2011; pp.369-370.
- 673 40. Gandham, S.; Dawande, M.; Prakashc, R. Link scheduling in wireless sensor networks: Distributed
674 edge-coloring revisited. *J. Parallel Distrib. Comput.* **2008**, *68*, 1122-1134.

